

The Single-degenerate Binary Origin of Tycho's Supernova as Traced by the Stripped Envelope of the Companion

F.J. Lu¹, Q.D. Wang², M.Y. Ge¹, J.L. Qu¹, X.J. Yang³, S.J. Zheng¹, and Y. Chen¹

¹*Key Laboratory for Particle Astrophysics, Institute of High Energy Physics, Chinese Academy of Sciences, Beijing 100049, P.R. China; lufj@mail.ihep.ac.cn*

²*Department of Astronomy, University of Massachusetts, Amherst, MA 01003, USA*

³*Faculty of Materials, Optoelectronics and Physics, Xiangtan University, Hunan 411105, P.R. China*

ABSTRACT

We propose that a non-thermal X-ray arc inside the remnant of Tycho's supernova (SN) represents the interaction between the SN ejecta and the companion star's envelope lost in the impact of the explosion. The X-ray emission of the remnant further shows an apparent shadow casted by the arc in the opposite direction of the explosion site, consistent with the blocking of the SN ejecta by the envelope. This scenario supports the single degenerate binary origin of Tycho's SN. The properties of the X-ray arc, together with the previous detection of the companion candidate and its space velocity by Ruiz-Lapuente et al. (2004) and Hernández et al.(2009), enables us to further infer 1) the progenitor binary has a period of $4.9_{-3.0}^{+5.3}$ days, 2) the companion gained a kick velocity of 42 ± 30 km s⁻¹, and 3) the stripped envelope mass is about $0.0016 (\leq 0.0083) M_{\odot}$. However, we notice that the nature of the companion candidate is still under debate, and the above parameters need to be revised according to the actual properties of the companion candidate. Further work to measure the proper motion of the arc and to check the capability of the interaction to emit the amount of X-rays observed from the arc is also needed to validate the current scenario.

Subject headings: ISM: supernova remnants—supernovae: general—supernovae: individual (Tycho's SN)

1. Introduction

While Type Ia supernovae (Ia SNe) play a fundamental role in cosmology and chemical evolution of the Universe, their exact origin remains greatly uncertain. One of the leading mechanisms for such a SN is the thermonuclear explosion of a white dwarf when its

mass reaches a critical value via accretion from a normal stellar companion in a binary, which is called the single-degenerate scenario (Whelan & Iben 1973; Wheeler et al. 1975; Nomoto 1982; Hillebrandt & Niemeyer 2000). This scenario is supported by the possible identification of the survived stellar companion of the Ia SN observed by Tycho Brahe in 1572 (Ruiz-Lapuente et al. 2004a), although little is yet known about the putative progenitor binary. A specific prediction of the single-degenerate scenario is that up to 0.5 solar mass can be stripped by the impact of Ia SN from its companion star (Wheeler et al. 1975; Fryxell & Arnett 1981; Taam & Fryxell 1984; Chugaj 1986; Marietta et al. 2000; Meng et al. 2007). So far, however, no direct observational evidence for the stripped envelope has been reported; only an upper limit of 0.01 solar mass has been set for two extragalactic Ia SNe (Leonard 2007). In comparison, stellar remnants are expected to be completely dispersed if a SN is due to the merger of two white dwarfs (the double-degenerate scenario; Iben & Tutukov 1984; Whelan & Iben 1973).

We select the Tycho supernova remnant (SNR) to search for the stripped material motivated by the detection of its candidate companion star (Tycho G, a G0-G2 type sub-giant), which shows a large peculiar velocity (Ruiz-Lapuente et al. 2004a; Hernández et al. 2009). This remnant is one of the two identified Galactic type Ia SNRs, as revealed by the light curve, radio emission, and X-ray spectra (Baade 1945; Baldwin 1957; Hughes 1995; Ruiz-Lapuente et al. 2004a). It is young (437 years), nearby (3 ± 1 kpc; de Vaucouleurs 1985), and of high X-ray brightness (Cassam-Chenaï et al. 2007). With the available deep observations from the Chandra X-ray Observatory (CXO), this remnant is an ideal laboratory to search for the stripped mass entrained in the ejecta.

2. Observation and Data Reduction

Table 1 lists the 12 CXO observations of the Tycho SNR used in this study. These observations were carried out by the ACIS-I, the imager array of the Advanced CCD Imaging Spectrometer (ACIS), with a field of view large enough to cover the whole remnant. The data were calibrated with the Chandra Interactive Analysis of Observations (CIAO V4.1) software package following the standard procedure to correct for charge-transfer inefficiency (CTI) effects and the time-dependence of the gain, to clean bad pixels, and to remove time intervals of background flares. The final total effective exposure for these observations is a little bit longer than 1 Ms.

3. Results

Fig. 1 shows the intensity images of the remnant in different energy bands. In the 4-6 keV band image (Fig. 1 (a)), which is dominated by non-thermal X-ray emission sensitive to shocks, which accelerate particles, there appears an intriguing arc (as marked in the figure), only about half way from the SN site (RA (2000) =00:25:23.8; DEC (2000) =64:08:04.7; Ruiz-Lapuente et al. 2004a) and is as bright, narrow, and sharp as those filaments at the outer boundaries of the remnant. This unusual arc was first noticed by Warren et al. (2005). They suggested that it may still be part of the SNR rim seen in projection. In comparison, Figs. 1 (b), (c), and (d) show the remnant in 1.6-2.0, 2.2-2.6, and 6.2-6.8 keV energy bands, representing the intensity distributions of Si, S, and Fe emission lines. We find that the Fe $K\alpha$ line emission is unusually faint in a cone just outside of the arc (in the direction away from the SN site), in comparison with the other regions beyond the same radius. The opening angle of this cone (about 20°) is similar to that of the arc relative to the SN site. In the same cone, especially at the outer rims of the SNR, the 4-6 keV continuum emission as well as the Si and S line intensities also appear to be relatively deficient, though not as obvious as in the Fe $K\alpha$ band. These relative intensity contrasts are shown quantitatively in Fig. 2 (a). On the other hand, Fig 2(b) shows the same intensity contrasts for region within the arc radius, where local peaks appear at nearly the same angular positions of the dips of the profiles outside the arc. Observing the images we find that the enhancements are very close to the arc. We interpret the intensity deficiency in the cone outside the arc and the local enhancements inside the arc as the blocking of the SN ejecta by the arc.

The spectrum of the arc is shown in Fig 3. The on-source spectrum is extracted from the region defined by the inner polygon in Fig. 1(a), while the background is from the region between the inner and outer polygons. Fig 3 shows obvious dips at the positions of the Si, S and Fe lines in the source spectrum obtained. Since the background thermal emission dominates the nonthermal emission at these energies, these dips are probably due to the clumpy distribution of the SN ejecta and so highly variable background thermal emission surrounding the arc. Fitting the source spectrum with a power law model gives a photon index of 2.45 ± 0.09 (90% confidence errors), an absorption column density of $(8.7 \pm 0.9) \times 10^{21} \text{ cm}^{-2}$, an unabsorbed 0.5-10 keV flux of $7.8 \times 10^{-13} \text{ erg cm}^{-2} \text{ s}^{-1}$, and χ^2 of 291 for 200 degrees of freedom. If we ignore the data in 1.6-2.0, 2.2-2.6 and 6.0-7.0 keV, which are probably effected by the over-subtraction of the background line emission, the fitted parameters are then photon index $2.47_{-0.08}^{+0.16}$, absorption column density $9.0_{-0.7}^{+1.4} \times 10^{21} \text{ cm}^{-2}$, and unabsorbed 0.5-10 keV flux $8.4 \times 10^{-13} \text{ erg cm}^{-2} \text{ s}^{-1}$, as well as a significantly improved χ^2 of 176 for 171 degrees of freedom. Therefore, we conclude that the arc is nonthermal.

4. The nature and origin of the X-ray arc

We find that the X-ray arc is most probably in the interior of the SNR instead of a (morphologically) unusual feature of the outer rim projected well inside the remnant. The sharp and bright appearance of the X-ray arc is similar to those of the filaments at the outer rim of the SNR (Cassam-Chenaï et al. 2007), implying that the arc is observed almost edge on. If it is in the out layer of the SNR and the observed small angular distance from the geometric centre is due to the projection effect, then the arc should be much more diffuse as it is observed half face on. In the 4-6 keV map, there exist some relatively bright features within the blast wave boundary. However, most of them are substantially more diffuse and coincide with bright thermal structures spatially, and none of them is as far away from the boundary as the arc is (see also Warren et al. 2005). The arc is convexed toward the SN site, which is opposite to those of the filaments at the outer boundary. Furthermore, larger and fainter filaments tend to run northward from the southeast (Warren et al. 2005) and bent outward. The morphology of the arc can be naturally produced by the interaction between the SN ejecta and a cloud. As will be discussed in the following, the arc most probably represents the materials stripped from the companion star by the SN explosion and is in the interior of the SNR.

First, the arc must be related to the progenitor system of the SN. If it is not related to the progenitor system, it should then represent a dense cold molecular cloud that has survived for long time. Actually, the milli-meter and optical observations suggest that the Tycho SNR is possibly interacting with molecular clouds at the northeastern and the southwestern rims (Lee et al. 2004; Ghavamian et al. 2000). These regions show strong 4-6 keV emission. However, neither CO nor optical emission enhancement has been detected to be spatially coincident with the X-ray arc. It is unlikely to be a molecular cloud.

Second, the arc cannot arise from the materials ejected by the progenitor binary system of the SN. Since the mass donor is suggested to be very similar to the Sun but a slightly evolved one (Ruiz-Lapuente et al. 2004), we don't expect that it could contribute to the cloud (e.g., via a stellar wind). One might think that a planetary nebula surrounding the exploded white dwarf could be a source of the cloud material. However, planetary nebulae always show a spherically or axially symmetric morphology. The singleness of the X-ray arc makes this possibility very unlikely.

Finally, and most probably, the matter generating the X-ray arc is stripped from the companion star during the SN explosion. Such a mechanism has been suggested by many theoretical works (Wheeler et al. 1975; Fryxell & Arnett 1981; Taam & Fryxell 1984; Chugai 1986; Marietta et al. 2000; Meng et al. 2007) although no direct observational evidence is currently available (Leonard 2004). Arguments for this mechanism are as follows: (1) The

stripped materials are confined in a small angular range, which can naturally explain the singleness of the arc; (2) The opening angle (about 20°) of the arc relative to the SN site (Ruiz-Lapuente et al. 2004), the absence of the X-ray line emission in the cone away from the arc, and the local enhancements of X-ray emission immediately within the arc radius are all well consistent with the ejecta blocking scenario of the stripped stellar envelope (Marietta et al. 2000); (3) The gas in the envelope of the companion star is expected to have a temperature of a few 10^3 K, it can not cool down to the CO emitting temperature in 400 years, especially in a hot environment; (4) The impact of the SN blast wave and ejecta on the stripped envelope will generate a shock wave, just like those represented by the nonthermal X-ray filaments at the outer rim, but with a smaller velocity because the envelope is denser than the surrounding ISM. The shock wave can accelerate electrons to emit the nonthermal X-rays. (5) The angle between the direction of the arc to the explosive centre and the proper motion velocity of Tycho G is well consistent with the theoretical predictions and simulations (Marietta et al. 2000; Ruiz-Lapuente et al. 2004; Meng et al. 2007), as detailed in the following.

5. Constraints on the progenitor binary system

The above interpretation together with the existing measurement of the companion’s present velocity gives tight constraints on properties of the progenitor binary of Tycho SN (see Fig. 4 for an illustration). Because of the SN impact, the companion star should receive a kick as well as the envelope stripping in the same direction and in the orbital plane of the progenitor binary. The direction should be perpendicular to the orbiting velocity of the companion as it is expected to be in a circular orbit just before the SN (Marietta et al. 2000; Meng et al. 2007). For Tycho G, the measured radial velocity is -50 ± 10 km s $^{-1}$ [with the projected Galactic rotation contribution (-30 ± 10 km s $^{-1}$) subtracted; Hernández et al. 2009], while the tangential one is -94 ± 27 km s $^{-1}$ (Ruiz-Lapuente et al. 2004a). Taking the uncertainty in the distance (3 ± 1 kpc; de Vaucouleurs 1985) into account, the tangential velocity is -94 ± 41 km s $^{-1}$. The projected angle between the stripping direction and the current velocity of Tycho G relative to the SN site is $\alpha = 63 \pm 13^\circ$, where the error accounts for the uncertainties in both the proper motion measurement and the arc/shadow central line (about 2°). Because the X-ray arc/shadow is viewed almost edge on (with an assumed uncertainty of 10°), the stripped velocity should be nearly perpendicular to the line of sight. Therefore, the real angle between the stripping (or the kick) and the velocity of Tycho G is $\beta = 67 \pm 16^\circ$. Numerical simulation by Marietta et al. (2000) shows that the ratio between the orbital velocity and kick velocity is from 2.3 to 11.2, and so the real angle between the kick and the space velocity of the stellar remnant is between 67° to 85° . Our result is consistent

with these predictions.

We can then infer that the companion had an orbital velocity (V_o) of 98 ± 36 km s⁻¹ in the progenitor binary, received a kick velocity (v_k) of 42 ± 30 km s⁻¹, and the inclination angle of the orbital plane is $31\pm 13^\circ$. We can also constrain the separation between the two stars in the progenitor binary with the formula $a = \frac{M_1^2 G}{(M_1 + M_2)V_o^2}$, where M_1 is the mass of the SN progenitor and is assumed to be 1.4 solar mass — the Chandrasekhar mass of a white dwarf, M_2 the mass of the companion star, and G the gravitational constant. Tycho G is similar to the Sun spectroscopically (Ruiz-Lapuente et al. 2004a; Hernández et al. 2009) and thus has a mass of about one solar or slightly higher (depending on the luminosity type; see below). We then estimate $a = \frac{1}{2.4+\varepsilon}(2.7\pm 2.0)\times 10^7$ km, where ε is the mass stripped from the companion and should be considerably smaller than one, hence negligible. The corresponding orbital period is then $4.9_{-3.0}^{+5.3}$ days. These orbital parameters and kick velocity are summarized in Table 2. They are well consistent with the theoretical predictions (Marietta et al. 2000; Meng et al. 2007). Pakmor et al. (2008) simulated the impact of type Ia SN on main sequence binary companions. They find that the kick velocity of the companion star after the impact of the SN ejecta varies from 17 to 61 km s⁻¹ for different models. Our results are also consistent with their simulations.

We may also check the evolutionary state of the companion, assuming that it filled the Roche lobe when the SN took place. Because the Roche lobe radius is (Paczynski 1971) $r_r = [0.38 + 0.2 \log(\frac{1+\varepsilon}{1.4})] \times [\frac{1}{2.4+\varepsilon}(2.7\pm 2.0)] \times 10^7 \approx (4.0\pm 2.7) \times 10^6$ km, about 5.7 times the solar radius, the companion should be a subgiant, fully consistent with the luminosity classification of Tycho G Ruiz-Lapuente et al. (2004a) and Hernández et al. (2009).

The angular size (about 20°) of the X-ray arc relative to the SN site is smaller than that subtended by the Roche lobe (40°), which may be expected from the compression and stripping of the envelope in the bow-shocked SN ejecta material (Fig. 4). The angular separation between the SN site and the arc is about half of the outer radius of the remnant, which presumably reflects the difference in their velocities. A type Ia SN explosion releases a typical kinetic energy of $(1-1.4)\times 10^{51}$ erg, and the mean ejecta velocity (v_{ej}) for a Chandrasekhar mass of $1.4 M_\odot$ is 8500-10000 km s⁻¹. The momentum conservation for the stripped mass (M_{str}), the kicked companion star, and the ejecta in the solid angle subtended by the envelope can be expressed as: $M_{ej}v_{ej} = (M_{ej} + M_{str})\frac{v_{ej}}{2} + M_c v_k$. Assuming a spherically symmetric SN and using a companion star mass of 1 solar, an ejecta velocity of 9230 km s⁻¹, and $v_k = 42$ km s⁻¹, as well as the 20° wide solid angle, we estimate the mass of the envelope to be $0.0016 M_\odot$. Taking the uncertainty of v_k (± 30 km s⁻¹) into account, the upper limit of the stripped mass is $0.0083 M_\odot$. The mass outside the assumed solid angle (e.g., to account for the full Roche lobe) should be negligible because of the expected highly-concentrated ra-

dial mass profile of a subgiant star (Meng et al. 2007). This estimation of the stripped mass is consistent with that observed for two extragalactic Ia SNe (Leonard 2007), significantly lower than the theoretical predictions by Marrieta et al. (2000) and Meng et al. (2007), and is close to (though still lower than) 1 to several percent that simulated by Pakmor et al. (2008).

Although the stripped mass is small, it is enough to produce the X-ray arc. Katsuda et al. (2010) estimated that the mean ambient density of Tycho’s SNR is 0.0015 cm^{-3} , or $<0.2 \text{ cm}^{-3}$. The mass of the ambient ISM in a cone of 20° radius should then be about $4 \times 10^{-5} M_\odot$, or $< 5 \times 10^{-3} M_\odot$, smaller than or at most comparable to the stripped mass. Since bright nonthermal filaments have been observed all along the rim of the remnant (e.g., Cassam-Chenai et al. 2007), the interaction between SN ejecta (probably denser at the arc position) and the stripped mass should be strong enough to be responsible of the X-ray arc emission.

Recently, Kerzendorf et al. (2009) have reported the new space velocity and mass measurements of Tycho G, which are different from those by Ruiz-Lapuente et al. (2004a). We list the new measurements and the corresponding binary parameters in Table 2. The new orbital radius and period are several times as those derived from Ruiz-Lapuente et al. (2004a) and Hernández et al. (2009). The angle between the kick and the space velocity of the stellar remnant is therefore about 82 degrees, only marginally consistent with the numerical simulations (Marietta et al. 2000). In the scheme of momentum conservation, the amount of the stripped mass is derived as $0.0087 \pm 0.0017 M_\odot$. It is higher than that from Ruiz-Lapuente et al. (2004a) and Hernández et al. (2009), but still consistent with the simulations by Pakmor et al. (2008) and the observations by Leonard (2007).

As pointed out by Kerzendorf et al. (2009), there is a simple relationship between the companion’s rotation velocity (v_{rot}) and its orbital velocity ($v_{orb,2}$): $v_{rot} = \frac{M_1 + M_2}{M_1} f(q) V_{orb,2}$, where $f(q)$ is the ratio of the companion’s Roche-lobe radius to the orbital separation and $q = M_1/M_2$ is the mass ratio of the primary to the companion at the time of the explosion. If M_2 is $0.3\text{-}0.5 M_\odot$ (Kerzendorf et al. 2009), v_{rot} of the companion’s surface should be about 24 km s^{-1} , much higher than 7.5 km s^{-1} , the upper limit of Tycho G’s rotation velocity ($v_{rot} \sin i$), where i is the inclination angle of the the orbital velocity. Using the inclination angle that we obtained in this paper, the upper limit of v_{rot} for Tycho G is about 10 km s^{-1} , still significantly lower than 24 km s^{-1} . Kerzendorf et al. (2009) proposed that a red giant scenario where the envelope’s bloating has significantly decreased the rotation could be consistent with their observation of the low rotation velocity. Since the effect of the inclination angle is small, Tycho G remains a stripped giant if it is the mass donor, as suggested by Kerzendorf et al. (2009).

If the companion is about $1 M_{\odot}$, its surface velocity was about 60 km s^{-1} at the SN explosion, as derived from the binary parameters listed in Table 2 and that it filled the Roche lobe, which has a radius of about $5.7 R_{\odot}$. However, the companion may have a radius of $1\text{-}3 R_{\odot}$ now (Ruiz-Lapuente et al. 2004a; Hernández et al. 2009), and so the surface velocity of the stellar remnant should be about $10\text{-}31 \text{ km s}^{-1}$, marginally consistent with the upper limit of v_{rot} observed by Kerzendorf et al. (2009) and the inclination angle that we obtained. We speculate that the decrease of the radius is possibly due to the destruction of the white dwarf. Before the SN explosion, the strong radiation of the accreting white dwarf inflated the envelope of the companion star to fill the Roche-lobe, and the radius of the companion star shrinks to $1\text{-}3 R_{\odot}$ now because the heating of the white dwarf does not exist. In addition, we note here that the shrink did not accelerate the rotation significantly, because the inflated envelope only contributes a small fraction of the total mass of the companion star and most of it was stripped away by the SN.

Using the position of the arc and the age of the remnant, we obtained a mean velocity of the arc outward from the SN site as about $0''.28 \text{ yr}^{-1}$. As measured by Katsuda et al. (2010), the Tycho’s remnant is expanding at a proper motion velocity around $0''.3 \text{ yr}^{-1}$, in contrast to the mean expansion speed of about $0''.55 \text{ yr}^{-1}$ from the radius and age of the remnant. This shows that the remnant are in a deceleration phase due to the interaction with the ISM. If the arc is a projected feature that is in the outer layer of the remnant, it should have a proper motion velocity of $\sim 0''.15 \text{ yr}^{-1}$. If the arc is actually about half way from the SN site and represents the interaction of the SN explosion and the stripped companion envelope, the proper motion should be quite close to the mean velocity $\sim 0''.28 \text{ yr}^{-1}$, as discussed below.

On one hand, the arc is unlikely in an accelerating phase. The binary separation is tiny compared to the distance of the X-ray arc from the SN site. Even the Fe ejecta, which is expected to have the lowest velocity and was measured as $\sim 3000 \text{ km s}^{-1}$ currently (Furuzawa et al. 2009), can pass such a separation within several hours. Most of the impact of the ejecta on the companion envelope (and thus the acceleration of the stripped mass) should take place soon after the explosion. On the other hand, the arc can not be significantly decelerated. Since the distance of the X-ray arc from the SN site is about half of the remnant radius, using the ISM density given by Katsuda et al. (2010), the ISM mass in the cone between the SN site and the X-ray arc is $\sim 5 \times 10^{-6} M_{\odot}$, much smaller than the stripped envelope mass. Although the ISM decelerates the motion of the stripped envelope material, it is quite insignificant given the small mass. Therefore, the stripped envelope went through a very short accelerating phase in the beginning of the SN explosion, and has remained in an almost free expansion state since then.

We have attempted to measure the proper motion of the X-ray arc so as to check the

above scenario, since the expected proper motion may be detectable at *Chandra*'s resolution. Unfortunately, the arc typically fallen more or less at a gap between two ACIS-I chips, especially in three early observations. In addition, the arc is heavily contaminated by strong thermal emission in the low energy band. In 4-6 keV, where nonthermal emission dominates, the counting statistics of the arc are typically not sufficient in early observations. As a result, we cannot yet get a reliable multi-epoch measurements of the arc positions to allow for a reliable determination of the proper motion. Future observations with more careful positioning of the arc in the detector and with a total exposure time comparable to the ACIS-I observations in 2009 will make such measurements feasible.

6. Summary

We have shown that a self-consistent single-degenerate binary model provides a natural and unified interpretation of the observed unique X-ray arc/shadow in the Tycho's SNR. Two sets of parameters of the progenitor binary system have also been presented using the optical observation results of the candidate companion star (Tycho G) obtained by Ruiz-Lapuente et al. (2004a) and Kerzendorf et al. (2009) respectively. The main points in favor of our interpretation are: (1) Although the nonthermal X-ray arc is half way from the remnant center, the high brightness show that it is viewed almost edge on and so unlikely a projected feature in the outer layer of the remnant. Together with its sharp inward convex shape, the arc most probably represents the interaction between the ejecta and a bulk of materials in the interior of the remnant. (2) This bulk of materials can not be due to a pre-existing molecular cloud or materials ejected by the progenitor binary system. The impact generating the X-ray arc is most likely between SN ejecta and the stripped envelop of the companion star. (3) The X-ray emission of the remnant shows an apparent shadow casted by the arc in the opposite direction of the explosion site, and there are local enhancements in the same direction immediately within the X-ray arc, consistent with the blocking of the SN ejecta by the envelope. (4) We obtained a stripped mass of $\leq 0.0083 M_{\odot}$, which is consistent with that observed for two extragalactic Ia SNe (Leonard 2007) and close to the recent simulations by Pakmor et al. (2008). (5) The angle between the motion of the companion candidate and the direction of the arc as well as the derived kick velocity of the companion star are well consistent with the theoretical predictions and the numerical simulation results.

However, we note that there are still several points that can not be well interpreted by the current scenario, and further work is needed to reveal the physical processes related to the nonthermal X-ray arc. (1) The properties of Tycho G and whether it is the stellar remnant of Tycho's SN are under debate (Ruiz-Lapuente et al. 2004a; Hernández et al. 2009;

Kerzendorf et al. 2009). If Tycho G is not the stellar remnant, the binary parameters and kick velocity obtained in this paper are unreliable anymore. Also, if Tycho G is the stellar remnant but has properties as obtained by Kerzendorf et al. (2009), the obtained angle between the kick and the space velocity of the stellar remnant is only marginally consistent with the numerical simulations (Marietta et al. 2000). (2) It has not been quantitatively estimated whether the interaction between the stripped envelope and the ejecta can produce shock wave strong enough to produce the nonthermal X-ray arc. (3) We failed to obtain a precise proper motion of the X-ray arc, which is an important criterion to differentiate the X-ray arc as inside the remnant from a projected feature in the outer layer. Further studies of the stellar remnant as well as the measurement of the proper motion velocity of the X-ray arc are therefore urged to check the validity of the scenario proposed in this paper.

Acknowledgments

We thank the referee for many insightful comments and suggestions that helped us greatly in the revision of the paper. This work is supported by National Basic Research Program of China (973 program, 2009CB824800) and by National Science Foundation of China (10533020 and 10903007). QDW acknowledges the support by CXC/NASA under the grant GO8-9047A and NNX10AE85G.

REFERENCES

- Baade, W.B. 1945, *ApJ*, 102, 309
- Baldwin, J.E., & Edge, D.O. 1957, *Observatory*, 77, 139
- Cassam-Chenaï, G., Hughes, J. P., Ballet, J., & Decourchelle, A. 2007, *ApJ*, 665, 315
- Chugaj, N. N. 1986, *AZh*, 63, 951
- de Vaucouleurs, D. 1985, *ApJ*, 289, 5
- Fryxell, B. A. & Arnett, W. D. 1981, *ApJ*, 243, 994
- Furuzawa, A. et al. 2009, *ApJ*, 693, L61
- Ghavamian, P., Raymond, J., Hartigan, P., & Blair, W.P. 2000, *ApJ*, 535, 266
- Hernández, J. I., Ruiz-Lapuente, P., Filippenko, A. V., et al. 2009, *ApJ*, 691, 1

- Hillebrandt, W. & Niemeier, J. C. 2000, ARA&A, 38, 191
- Hughes, J. P. et al. 1995, ApJ, 444, L81
- Iben, I. Jr. & Tutukov, A. V. 1984, ApJS, 54, 335
- Katsuda, S. et al. 2010, ApJ, 709, 1387
- Kerzendorf, W.E. et al. 2009, ApJ, 701, 1665
- Lee, J.J., Koo, B.C., & Tatematsu, K.C. 2004, ApJ, 605, L113
- Leonard, D. C. 2007, ApJ, 670, 1275
- Marietta, E., Burrows, A. & Fryxell, B. A. 2000, ApJS, 128, 615
- Meng, X., Chen, X. & Han, Z. 2007, PASJ, 59, 835
- Nomoto, K. 1982, ApJ, 253, 798
- Paczynski, B. 1971, ARA&A, 9, 183
- Pakmor, R., Röpke, F.K., Weiss, A., & Hillebrandt, W. 2008, A&A, 489, 943
- Ruiz-Lapuente, P. et al. 2004a, Nature, 431, 1069
- Ruiz-Lapuente, P. 2004b, ApJ, 612, 357
- Taam, R. E. & Fryxell, B. A. 1984, ApJ, 279, 166
- Warren, J.S. et al. 2005, ApJ, 634, 376
- Whelan, J. & Iben, I. Jr. 1973, ApJ, 186, 1007
- Wheeler, J. C., Lecar, M. & McKee, C. F. 1975, ApJ, 200, 145

Table 1. The Chandra/ACIS-I observations of the Tycho SNR

ObsID	Start Date	Exposure (ks)
3837	2003-04-29	145
7639	2007-04-23	109
8551	2007-04-26	33
10093	2009-04-13	118
10094	2009-04-18	90
10095	2009-04-23	173
10096	2009-04-27	106
10097	2009-04-11	107
10902	2009-04-15	40
10903	2009-04-17	24
10904	2009-04-13	35
10906	2009-05-03	41

Table 2. The measurements of Tycho G and the binary parameters of Tycho SN’s progenitor

Measurements	Ruiz-Lapiente04	Kernzendorf09
Proper motion (mas yr ⁻¹)	$\mu_l = -2.6 \pm 1.34$ $\mu_b = -6.11 \pm 1.34$	$\mu_l = -1.6 \pm 2.1$ $\mu_b = -2.7 \pm 1.6$
Tangential velocity (km/s)	94±41	51±28
Radial velocity (km/s)	50±10	49±10
Companion mass (M_\odot)	1.0	0.3-0.5
Orbital velocity (km/s)	98±36	71±16
Orbital period (Day)	4.9 ^{+5.3} _{-3.0}	28±26
Separation (10 ⁷ km)	1.1±0.7	3.2±0.6
Inclination angle (°)	31±13	47±20
Kick velocity (km/s)	42±30	23±20
Stripped Mass (M_\odot)	0.0016 (<0.0083)	0.0087±0.0017

Note. — The velocity and mass values of Ruiz-Lapiente04 were taken from Ruiz-Lapiente et al. (2004) and Hernández et al. (2009), and these of Kernzendorf09 were from Kernzendorf et al. (2009). The uncertainties of all the adopted and derived parameters in this table are at 1 σ confidence level.

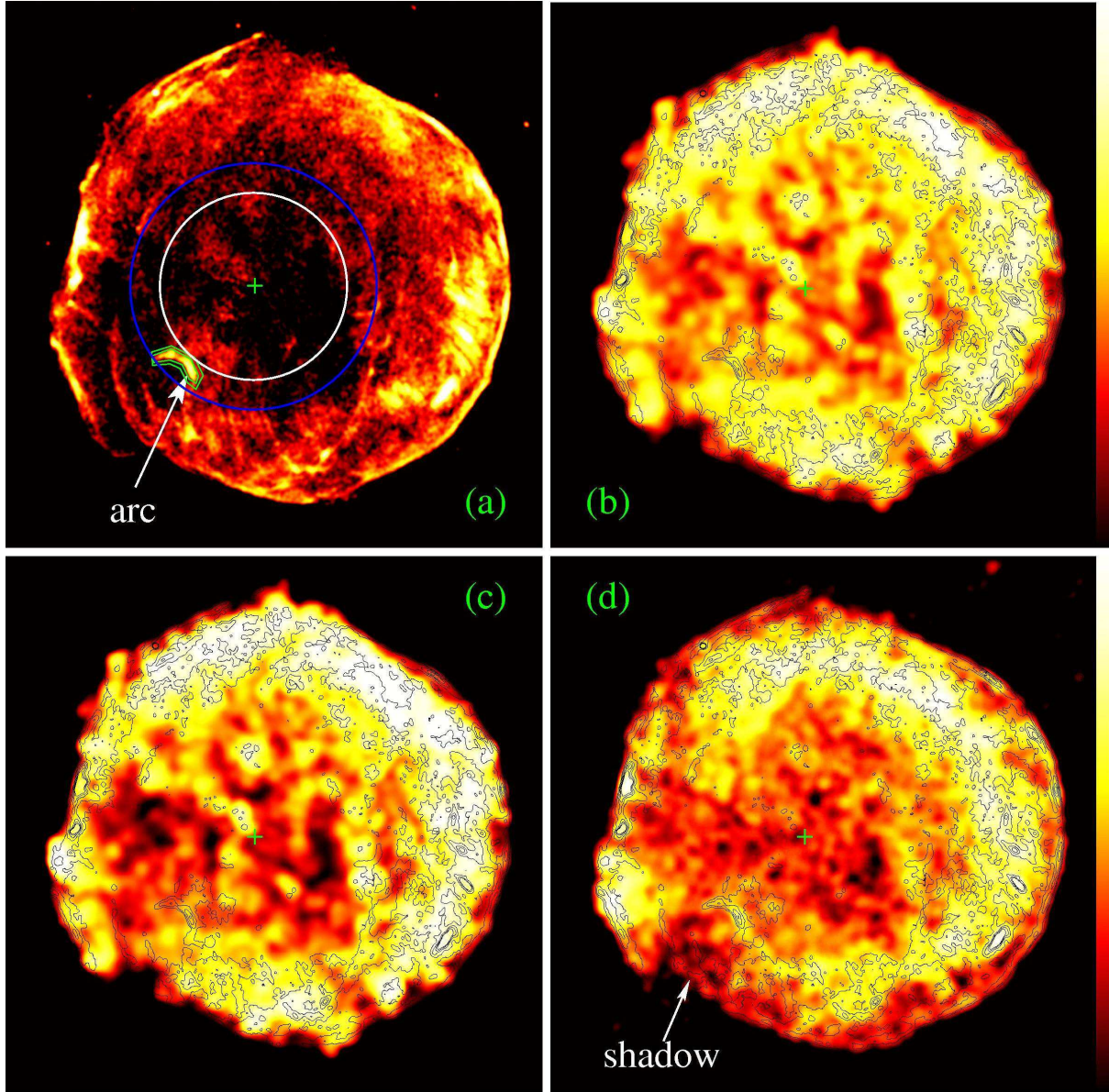


Fig. 1.— ACIS-I intensity images of the Tycho SNR in the 4-6 keV (a), 1.6-2.0 keV (b), 2.2-2.6 keV (c) and 6.2-6.8 keV (d) bands, which represent the nonthermal continuum, Si, S, and Fe emission distributions respectively. The images has been Gaussian-smoothed with the FWHM=3.5'' for (a) and 7.4'' for (b), (c), and (d). The colour changes logarithmically from 7.4×10^{-6} to 1.5×10^{-4} counts $\text{cm}^{-2} \text{s}^{-1} \text{arcmin}^{-2}$ for (a), 1.5×10^{-4} to 5.9×10^{-3} counts $\text{cm}^{-2} \text{s}^{-1} \text{arcmin}^{-2}$ for (b), 7.4×10^{-5} to 1.5×10^{-3} counts $\text{cm}^{-2} \text{s}^{-1} \text{arcmin}^{-2}$ for (c), and 2.2×10^{-6} to 3.0×10^{-5} counts $\text{cm}^{-2} \text{s}^{-1} \text{arcmin}^{-2}$ for (d). The contour levels represent the 4-6 keV emission and correspond to 1.5×10^{-5} , 3.0×10^{-5} , 8.9×10^{-5} , and 1.2×10^{-4} counts $\text{cm}^{-2} \text{s}^{-1} \text{arcmin}^{-2}$, respectively. The images are produced from 12 ACIS-I observations listed in Table 1, the green crosses denote the supernova explosion site inferred from the proper motion of Tycho G (Ruiz-Lapuente et al. 2004a), the blue (white) circle defines the inner (outer) boundary of the region from which the azimuth mean brightness profiles in the left (right) panel of Fig. 2 were produced.

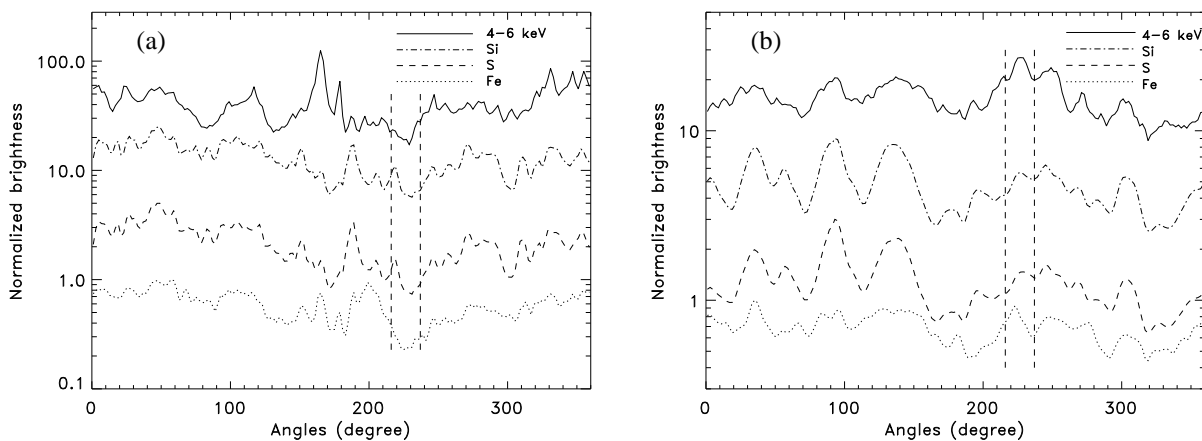


Fig. 2.— (a): The azimuth mean brightness profiles of the Tycho SNR beyond the radius of the X-ray arc in different energy bands as in Fig 1. Region used to produce the mean brightness profiles is between the blue circle (Fig 1 (a)) and the outer boundary of the remnant. The maximum values of the Fe, S, Si, and 4-6 keV curves were normalised to 1, 5, 25, and 125 so as to be displayed more clearly. The angular range shadowed by the X-ray arc is between the two vertical dashed lines. The angle is defined from west counter clock-wisely. (b): The same azimuth mean brightness profile of the Tycho SNR as in the left panel but for regions “inside” the X-ray arc radius, i.e., within the white circle. The maximum values of the Fe, S, Si, and 4-6 keV curves were normalised to 1, 3, 9, and 27 for the same reason as in (a).

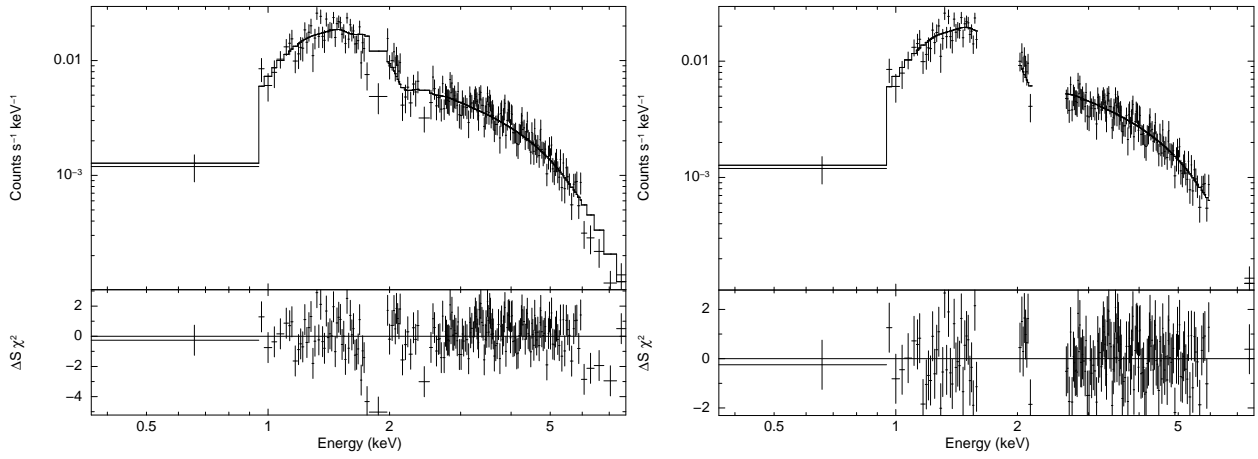


Fig. 3.— Chandra ACIS spectrum of the X-ray arc, together with a power law model fit as described in the text. In the spectral analysis, the background extracted from a region immediately surrounding the X-ray arc has been subtracted.

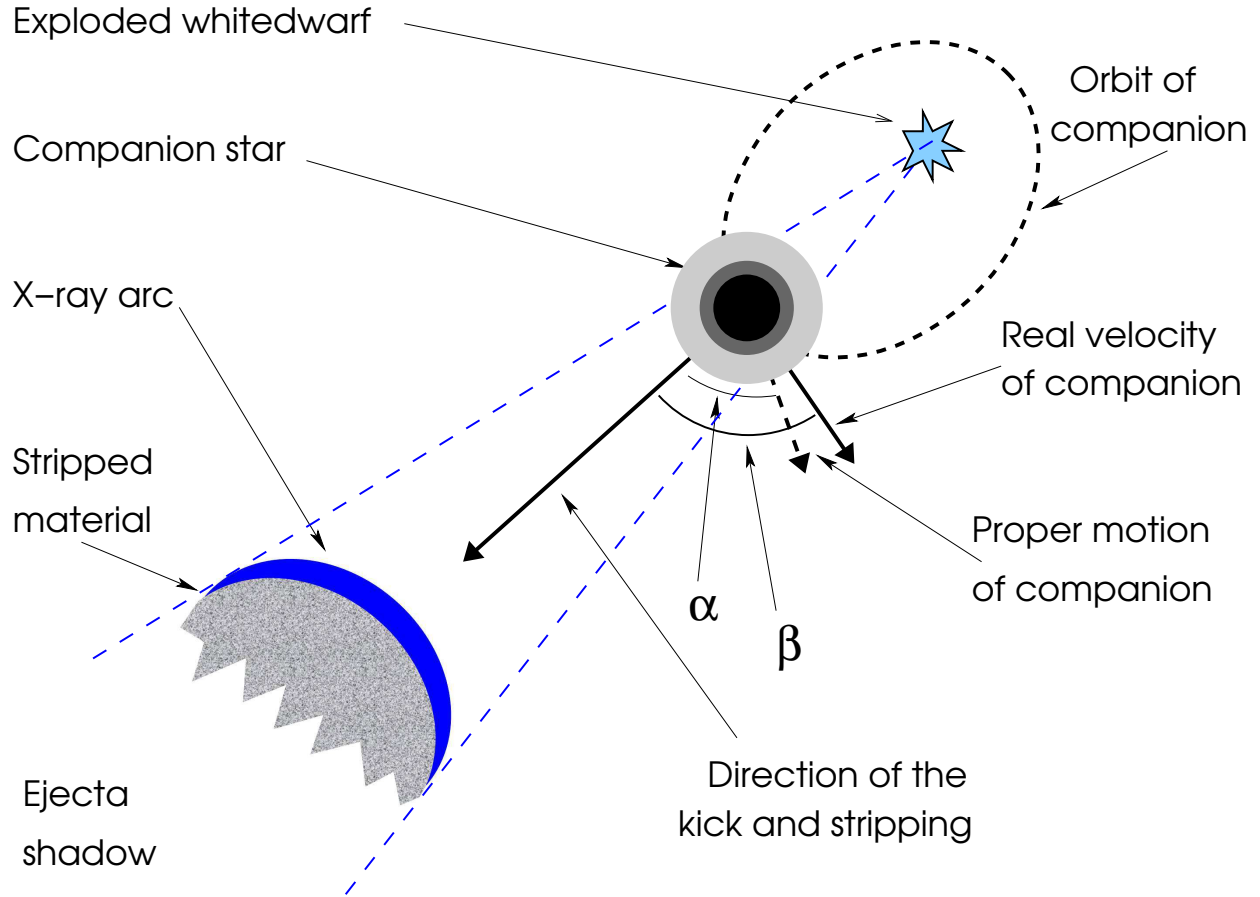


Fig. 4.— Illustration of the progenitor binary and the impact of the SN on the companion star. The companion star gained a kick in addition to the original orbital motion. Therefore, the angle between the kick direction and the companion star velocity has a projected (observed) value $\alpha = 63^\circ$, but is $\beta (= 67^\circ)$ in real space. The outer envelop of the companion star is stripped by the fast expanding SN ejecta in the same direction as the kick. The observed X-ray arc represents the shock wave generated by the interaction between the stripped envelope and the ejecta, which are behind the X-ray arc. The blocking of the stripped envelope produces a cone that is deficient of SN ejecta.